Drug Design, Development and Therapy

Dovepress
Taylor & Francis Group

Open Access Full Text Article

ORIGINAL RESEARCH

Inhibition of Colorectal Cancer by Perillaldehyde Through Targeting SRD5A1 to Induce Autophagy via the PI3K/AKT Pathway

Zhuyun Leng[1,*], Yiqian Zhang[2,*], Mingming Guo[3], Yan Chen[4], Zhiyong Wang[2]

[1]Endoscopy Center, Department of Gastroenterology, Shanghai East Hospital, School of Medicine, Tongji University, Shanghai, 200120, People's Republic of China; [2]Xiangan Hospital Xiamen University, China, School of Medicine, Xiamen University, Xiamen, 361100, People's Republic of China; [3]Naval Medical University, Shanghai, 200433, People's Republic of China; [4]Department of Pharmacy, Xiamen Susong Hospital, Xiamen, 361100, People's Republic of China

*These authors contributed equally to this work

Correspondence: Zhiyong Wang, Xiang'an Hospital of Xiamen University, School of Medicine, Xiamen University, Xiamen, 361100, People's Republic of China, Email cywangzhiyong@126.com; Yan Chen, Department of Pharmacy, Xiamen Susong Hospital, Xiamen, 361100, People's Republic of China, Email wzychenyan@126.com

Background: Colorectal cancer (CRC) is the third most common cancer globally, with treatment challenges persisting. Perillaldehyde (PAH), a major active monomer extracted from Perilla, has shown potential against CRC, though its mechanisms remain unclear. This study aims to assess the therapeutic potential of PAH against CRC and to clarify its mechanisms of action, providing a rationale for PAH as a promising candidate for anti-CRC therapy.

Methods: In vitro, we used CCK-8, colony formation, EdU assays, flow cytometry, and Western blotting to assess the effects of PAH on CRC cell proliferation and apoptosis. In vivo, a subcutaneous xenograft mouse model was established to evaluate the anti-CRC efficacy of PAH. Transcriptomic analysis was performed to identify possible mechanisms, particularly related to autophagy, and validated through TEM, immunofluorescence, Western blotting, and inhibitor assays. SRD5A1 was predicted as a potential target using Swiss Target Prediction and confirmed by molecular docking, molecular dynamics simulation, and CETSA. Bioinformatics analysis further assessed the clinical relevance and mechanism of SRD5A1, which was validated using a selective inhibitor.

Results: PAH demonstrated inhibitory effects on CRC in both experimental models. RNA-seq and experimental validation suggest that PAH may inhibit CRC by modulating the PI3K/AKT pathway to induce autophagy. Bioinformatics analysis indicates that SRD5A1 could be a potential target of PAH, with PAH treatment reducing SRD5A1 levels and enhancing autophagic activity through PI3K/AKT suppression.

Conclusion: PAH appears to inhibit CRC by targeting SRD5A1, thereby promoting autophagy through the PI3K/AKT pathway. This offers new perspectives for both the diagnosis and treatment of CRC.

Keywords: perillaldehyde, colorectal cancer, autophagy, PI3K/AKT pathway, SRD5A1

Introduction

CRC is one of the most common gastrointestinal malignancies. Its incidence and mortality have increased every year, taking 9.2% of the total deaths in the world annually.[1] Forecasts indicate a rise in worldwide CRC cases to 2.5 million by 2035.[2] Indeed, besides genetic predisposition, poor diet, smoking, obesity, and lack of physical activity in daily routine have also been established as key modifiable lifestyle factors contributing to the development of CRC.[3–5] In clinical settings, therapeutic interventions for CRC basically include conventional surgery, radiotherapy, and chemotherapy,[6] there is an urgent need for their alternatives, which should be more effective and safer.

The PI3K/AKT signaling pathway is a major oncogenic pathway implicated in various types of cancer.[7] It governs several cancer hallmarks, including cell survival, proliferation, metabolism, and metastasis. In CRC, dysregulation of the PI3K/AKT pathway is a common event. Among its core components, mutations in the PIK3CA gene—which encodes

Received: 10 March 2025
Accepted: 15 July 2025
Published: 28 July 2025

Graphical Abstract

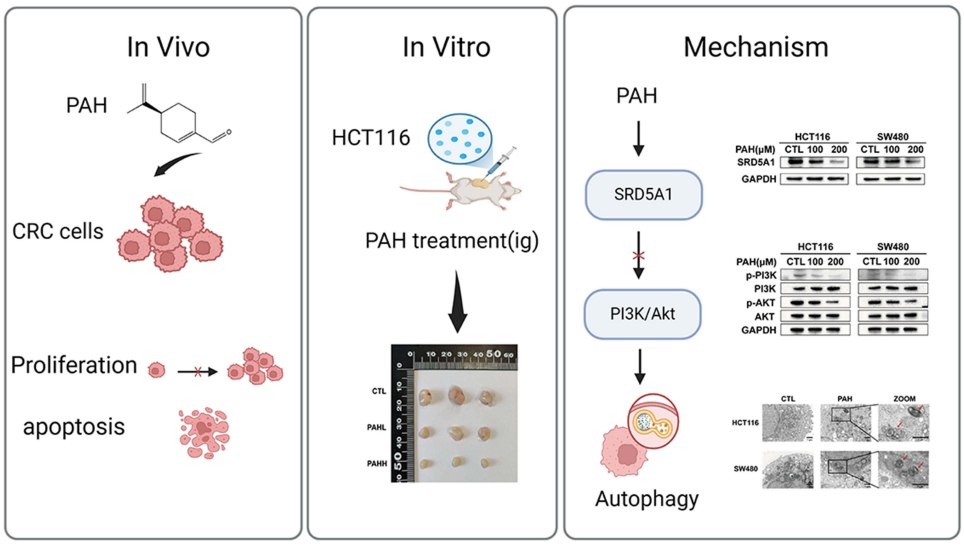

the catalytic subunit p110α of PI3K—are observed in approximately 10–15% of CRC cases.[8] These mutations lead to sustained activation of AKT, thereby promoting cell survival and uncontrolled proliferation. Furthermore, the PI3K/AKT pathway often exhibits crosstalk with other oncogenic cascades, such as the Wnt/β-catenin pathway, further enhancing malignant transformation. Activation of PI3K/AKT signaling has been linked to multiple aspects of cancer progression, including increased resistance to apoptosis, enhanced angiogenesis, and metastatic potential. Additionally, this pathway plays a role in modulating the tumor microenvironment and immune response, influencing interactions between cancer cells and surrounding tissues.[9] Therefore, understanding the regulation and therapeutic targeting of the PI3K/AKT pathway is critical for developing novel strategies against CRC.

The highly conserved degradative mechanism of autophagy is implicated in a wide range of physiological and pathological processes.[10,11] Autophagy has been associated with cancer, having functions related to both the promotion of tumor proliferation and death of cancer cells.[12] In CRC, autophagy is an important regulator of genomic stability, apoptosis cellular ecosystem, inflammation, and immune responses that are connected with the disease process.[13] One important aspect of oncology involves the PI3K/AKT pathway, an important autophagy inhibitor.[14] Developing a means to advance autophagy and thereby provoke apoptosis has become a viable approach to the treatment of cancer.[15] Therapeutic development based on small molecule drugs that target autophagic processes is thus a very promising strategy in the management of CRC.

SRD5A1 (steroid 5-alpha reductase type I) is a key enzyme involved in steroid metabolism and the regulation of sex hormone levels. Overexpression of SRD5A1 has been reported in various cancers, including breast, prostate, and non-small cell lung cancer, suggesting its potential role in tumorigenesis. Recent studies have identified SRD5A1 as a potential driver gene in CRC progression and proposed it as a novel biomarker.[9] Through bioinformatics analysis, we identified SRD5A1 as a likely molecular target of PAH. Furthermore, emerging evidence indicates that SRD5A1 may regulate cancer cell proliferation, apoptosis, and autophagy via modulation of the PI3K/AKT signaling pathway. However, its specific role in CRC remains largely unexplored, and no small-molecule inhibitors targeting SRD5A1 have been evaluated in this context. Based on these findings, we hypothesized that PAH may exert its anti-CRC effects by targeting SRD5A1, which we sought to validate in the present study.

Perilla has extensive pharmacological actions due to its extracts,[16] especially PAH, which is considered a major monoterpene and an essential oil from perilla; it is known for anti-inflammatory, antioxidant, antifungal, anticancer,

vasodilatory, anti-atherosclerotic, lipid-reducing, and cell cycle-inhibiting activities.[17–21] Yet, the exact mechanisms through which PAH impacts CRC remain unexplored.

The present study has evaluated anti-CRC properties of PAH by methodologies at both in vivo and in vitro levels. Our data showed that the interplay between PAH and the PI3K/AKT pathway promotes autophagy in CRC cells. Meanwhile, we identified steroid 5α-reductase 1 (SRD5A1) as a potential molecular target for PAH. We hereby greatly enrich the ongoing studies about PAH as an anti-CRC agent and substantiate further structural modifications.

Materials and Methods

Cell Lines and Cell Culture

Shanghai East Hospital supplied the human colon epithelial cells NCM460, human CRC cell lines HCT116 and SW480. For their propagation, the HCT116 and SW480 lines were cultured in Dulbecco's Modified Eagle Medium (Gibco, USA) supplemented with 10% fetal bovine serum (Gibco, USA) and 1% penicillin-streptomycin. The NCM460 cells, on the other hand, were cultured in Roswell Park Memorial Institute 1640 media (Gibco, USA). Under carefully regulated conditions, all cell types were grown at 37°C with 5% CO_2.

Cell Viability Assay

PAH (CAS: 18031–40-8), acquired from MCE (New Jersey, USA), was dissolved in DMSO (400 mM). The CCK-8 assay was used to measure the cell viability. Over the course of 24 or 48 hours, cells were exposed to different doses of PAH (0, 50, 100, 200, 400 μM) after being seeded at 2×10^3 cells per well in 96-well plates. Ten microliters of CCK-8 solution (Beyotime, Shanghai, China) was added to every well after exposure, and then incubated at 37°C for two hours. We used a microplate reader to measure viability at 450 nm, and GraphPad Prism 9.0 was used to obtain IC_{50} values. Each group comprised five subwells (n=5), and the experiment was independently repeated three times (n=3 independent experiments).

Colony Formation Assay

1×10^3 cells per well in 6-well plates was used to plate cells from the HCT116 and SW480 lines. Fresh medium was added to the medium after cell attachment and PAH was added 0, 100, and 200 μM for a period of 24 hours. Cells were fixed with 4% paraformaldehyde (Beyotime, Shanghai, China) for 20 minutes and stained with 0.1% crystal violet for 15 minutes after an additional 7–10 days of growth. Image J was used to count the colonies. Each experiment was repeated independently three times (n=3 independent experiments).

EdU-DNA Synthesis Assay

Confocal dishes were used to measure the cells' proliferative ability with the BeyoClick™ EdU-488 Cell Proliferation Assay Kit (Beyotime, Shanghai, China). Following a 24-hour treatment with PAH, cells underwent a 2-hour incubation with 10 μM EdU. Nuclei were then stained with Hoechst 33342 for 10 minutes, and cellular examination was performed using a Leica confocal microscope. Each experiment was repeated independently three times (n=3 independent experiments).

Flow Cytometry

Apoptosis detection was carried out using the Annexin V-FITC/PI kit (MultiSciences, Hangzhou, China) to assess apoptotic reactions to PAH. For 24 hours, HCT116 and SW480 cells were exposed to PAH (0, 100, 200 μM) after being cultivated in 6-well plates at 1×10^3 cells per well. Post-treatment, cells were stained according to the kit's guidelines with PI and Annexin V-FITC and analyzed for apoptosis using a BD FACSAria II flow cytometer. Each experiment was repeated independently three times (n=3 independent experiments).

Western Blot (WB)

The cells were fixed with a cell scraper after two ice-cold PBS washes. They were then lysed in RIPA buffer, which had been supplemented with 2% inhibitors of protease and phosphatase (Beyotime, Shanghai, China). A BCA test kit (Beyotime,

Shanghai, China) was used to extract and quantify proteins. Proteins were transferred onto PVDF membranes after being exposed to SDS-PAGE. After one hour of blocking with 5% skim milk, the membranes were probed with primary antibodies and left to overnight at room temperature. The next day, they were probed with secondary antibodies. Detection employed the Super Sensitive ECL luminescence reagent (Meilunbio, Dalian, China). Utilized antibodies were: Bax (1:1000. ZEN-BIOSCIENCE, #380709), Bcl-2 (1:1000. ZEN-BIOSCIENCE, #381702), PI3 Kinase p85α (1:1000, Abcam, ab182651), p-PI3 Kinase p85α (1:1000. ZEN-BIOSCIENCE, #341468), AKT (1:2000. Proteintech, #10176-2-AP), p-AKT (Ser 473) (1:1000. ZEN-BIOSCIENCE, #381555), SQSTM1/p62 (1:1000. ZEN-BIOSCIENCE, #380612), LC3B (1:1000. ZEN-BIOSCIENCE, #382687), SRD5A1 (1:1000, Proteintech, #66329-1-Ig), GAPDH (1:10000. Proteintech, #60004-1-Ig). Each experiment was repeated independently three times (n=3 independent experiments).

Immunofluorescence (IF) Analysis

Cells were planted on confocal dishes and treated with various doses of PAH. After 20 minutes of fixation in 4% paraformaldehyde, cells were permeabilized with 0.3% Triton X-100 (Beyotime, Shanghai, China). Then, for 10 minutes, the cells were blocked with QuickBlockTM Immuno Staining Block Solution (Beyotime, Shanghai, China). After exposing cells to an LC3B antibody for one night at 4°C, they were incubated in the dark for one hour before being processed with a secondary antibody labeled with Alexa Fluor 488 (Beyotime, Shanghai, China). Prior to examining the nuclei using laser confocal microscopy, the nuclei were stained with DAPI (Beyotime, Shanghai, China) and a fluorescence quenching agent (Beyotime, Shanghai, China) was added. Each experiment was repeated independently three times (n=3 independent experiments).

RNA-Seq

Following a 24-hour exposure to 0, 100, and 200 μM PAH, RNA was extracted using TRIzol reagent from three separate HCT116 cell types. The Illumina Novaseq6000 platform was used to sequence the libraries constructed from this RNA, resulting in 150bp paired-end reads. Each experiment was repeated independently three times (n=3 independent experiments).

Molecular Docking

PAH's 3D structure was sourced from the AlphaFold Protein Structure Database. Docking simulations were carried out with AutoDock1.5.7, and the results were visualized using PyMOL2.5.4.

Molecular Dynamics Simulation

Starting with the optimal conformation from molecular docking, simulations were conducted using GROMACS (V2020.3), applying AMBER99SB force field parameters and the SPC/E water model for solvation; sodium ions were used to neutralize the charge. The system underwent energy minimization with steepest descent and conjugate gradient methods, followed by equilibration at 300 K in NVT for 2000 ps and in NPT for another 2000 ps. A 50 ns simulation was performed, recording data every 10 ps, with system stability assessed by root mean square deviation (RMSD) analysis.

Bioinformatics Analysis

The GEPIA2 database was used to assess the differential gene expression between normal tissues and colon cancer (COAD). A log fold change (|Log2FC|) limit of 1 and a p-value of 0.01 were used, and data from the TCGA normal and GTEx studies were aligned.

Animal Experiment

From Changzhou Cavens Animal Experiment Company, we obtained eighteen male NXG mice defective in immunology, which were 6–8 weeks old. With approval number XMULAC20240001, this study complied fully with the ethical guidelines established by Xiamen University's Ethics Committee. A density of 1×10^7 cells per mouse of HCT116 was administered subcutaneously to each of the eighteen mice. Mice were divided into three groups at random and given oral dosages of PAH (100 mg/kg or 200 mg/kg) for 21 days in a row once their tumors reached a certain size. The volume of the tumors and the mice's body weight were measured every three days. When the treatment was complete, the mice were put down, and their tumors were removed, photographed, and then kept in 4% paraformaldehyde for further study.

HE Staining

4 μm slices were cut from tumor tissues that had been fixed in paraffin. An HE staining kit (Beyotime, Shanghai, China) was used to stain these sections, and a Motic EasyScan (Xiamen, China) was used for analysis.

Immunohistochemistry (IHC) Staining

Antigen retrieval was performed on deparaffinized tumor sections by rehydrating them in citrate buffer (pH 6.0). The next step was to incubate them at 4°C overnight with primary antibodies against Ki67 and PCNA. After that, they were exposed to an HRP-labeled secondary antibody for 1 hour. The DAB technique was employed for detection.

Statistical Analysis

Using GraphPad Prism 9.0, the data underwent statistical evaluation and are displayed as mean ± standard deviation (SD). The *t*-test was utilized to determine differences between two groups, while comparisons involving more than two groups were conducted using one-way ANOVA. Statistical significance was recognized for $p<0.05$. *P < 0.05, **P < 0.01, ***P < 0.001, ****P < 0.0001.

Results

PAH Inhibits the Proliferation of CRC Cells

The preliminary study employed the CCK-8 assay to assess the effects of different PAH (Figure 1A) concentrations on the viability of human CRC cells over a 24-hour period. As demonstrated in Figure 1B, PAH reduced cell viability in a manner that is dependent on concentration. The IC_{50} values were established at 239.4 μM for HCT116 and 218.9 μM for SW480. In contrast to CRC cells, NCM460 cells showed no cytotoxicity at 200 μM PAH with an IC50 of 576.9 μM (Supplementary Figure 1A), highlighting the compound's selectivity for CRC cells. Further evaluations using colony

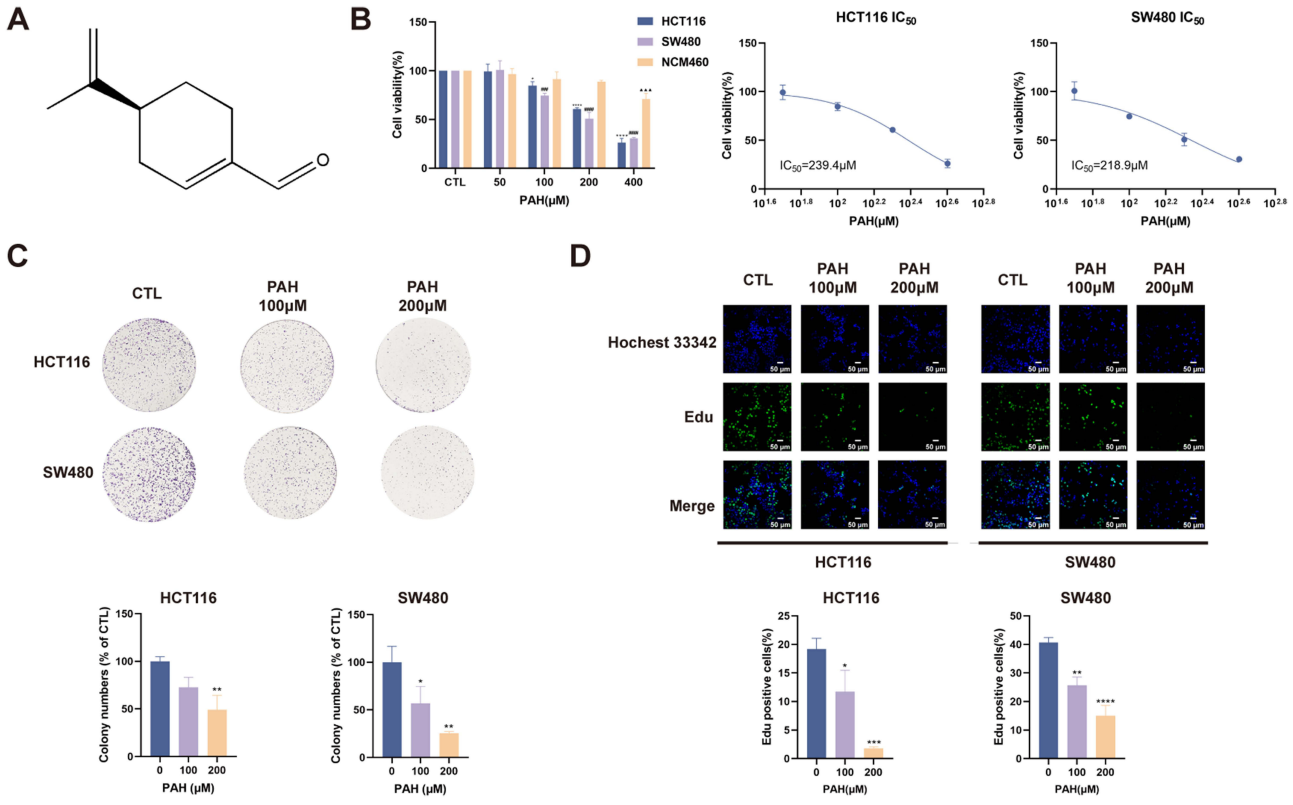

Figure 1 PAH inhibits the proliferation of CRC cells. (**A**) Structural representation of PAH. (**B**) Viability of cells determined by the CCK-8 kit post 24-hour PAH treatment. (**C**) Colony formation assay conducted on HCT116 and SW480 with designated PAH concentrations. (**D**) EdU-DNA synthesis assay was carried out in HCT116 and SW480 with different concentrations of PAH for 24h. Scale bar, 50 μm. All data were expressed as mean ± SD. *P < 0.05, **P < 0.01, ***P < 0.001, ****P < 0.0001.

https://doi.org/10.2147/DDDT.S525006

formation and EdU assays indicated a marked decrease in both colony numbers and EdU-positive cell proportions in SW480 and HCT116 cells following 24 hours of PAH treatment (Figure 1C and D).

PAH Induces Apoptosis of CRC Cells

We subsequently assessed the potential of PAH to trigger apoptosis in CRC cell lines. The process was observed through PI-Annexin V staining and flow cytometry, revealing a dose-dependent increase in apoptosis rates with PAH exposure (Figure 2A). WB analyses demonstrated a significant decrease in Bcl-2 protein levels alongside an elevation in BAX protein levels after PAH treatment (Figure 2B).

PAH Inhibits the Progression of CRC in Xenograft Mice Models

Research was carried out to examine the capacity of PAH to inhibit tumor growth in vivo, utilizing HCT116 xenograft models that received oral administrations of PAH at doses of 100 mg/kg and 200 mg/kg. The findings demonstrated a notable decrease in tumor growth rates within the PAH-treated cohort when juxtaposed with the control group throughout the duration of the study (Figure 3A, B and D). Notably, no adverse effects on mouse body weight were observed (Figure 3C). HE staining indicated a decrease in tumor cell density and structural disruption in the treatment group (Figure 3E). IHC analysis of Ki67 and PCNA expression also showed decreased levels in the treated group versus controls (Figure 3F).

RNA-Seq Analysis Predicts the Potential Mechanisms of Action of PAH

RNA-seq was utilized to investigate gene expression in HCT116 cells after 24 hours of treatment with PAH, with the goal of identifying potential anti-CRC mechanisms. Kyoto Encyclopedia of Genes and Genomes (KEGG) analysis indicated that pathways such as ferroptosis, p53, and the PI3K/AKT might be involved in PAH's anticancer effects

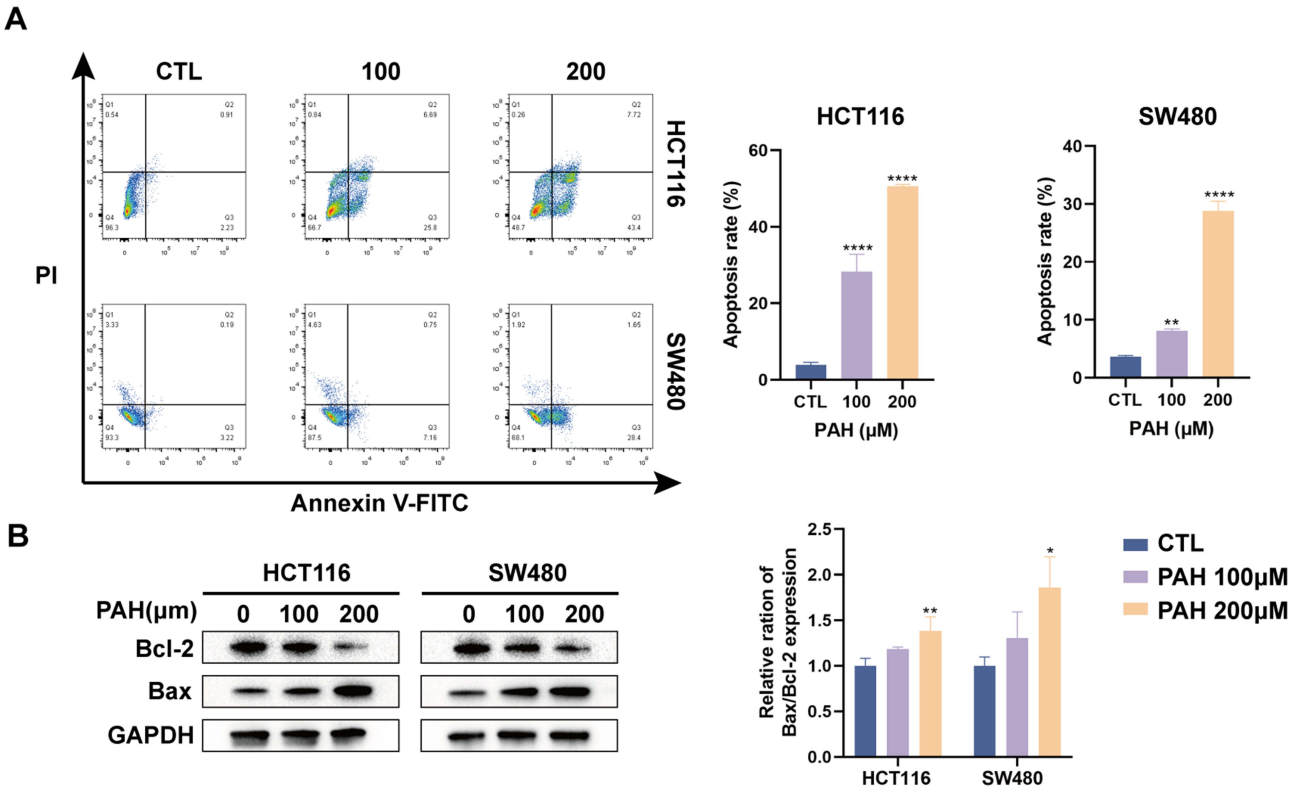

Figure 2 PAH induces apoptosis in CRC cells. (**A**) Apoptosis rates in HCT116 and SW480 cells were determined by flow cytometry following 24 hours of PAH treatment using Annexin V-FITC/PI double staining. (**B**) WB analysis tracked changes in Bcl-2 and BAX protein expression post-PAH treatment. All data were expressed as mean ± SD. *P < 0.05, **P < 0.01, ****P < 0.0001.

 https://doi.org/10.2147/DDDT.S525006

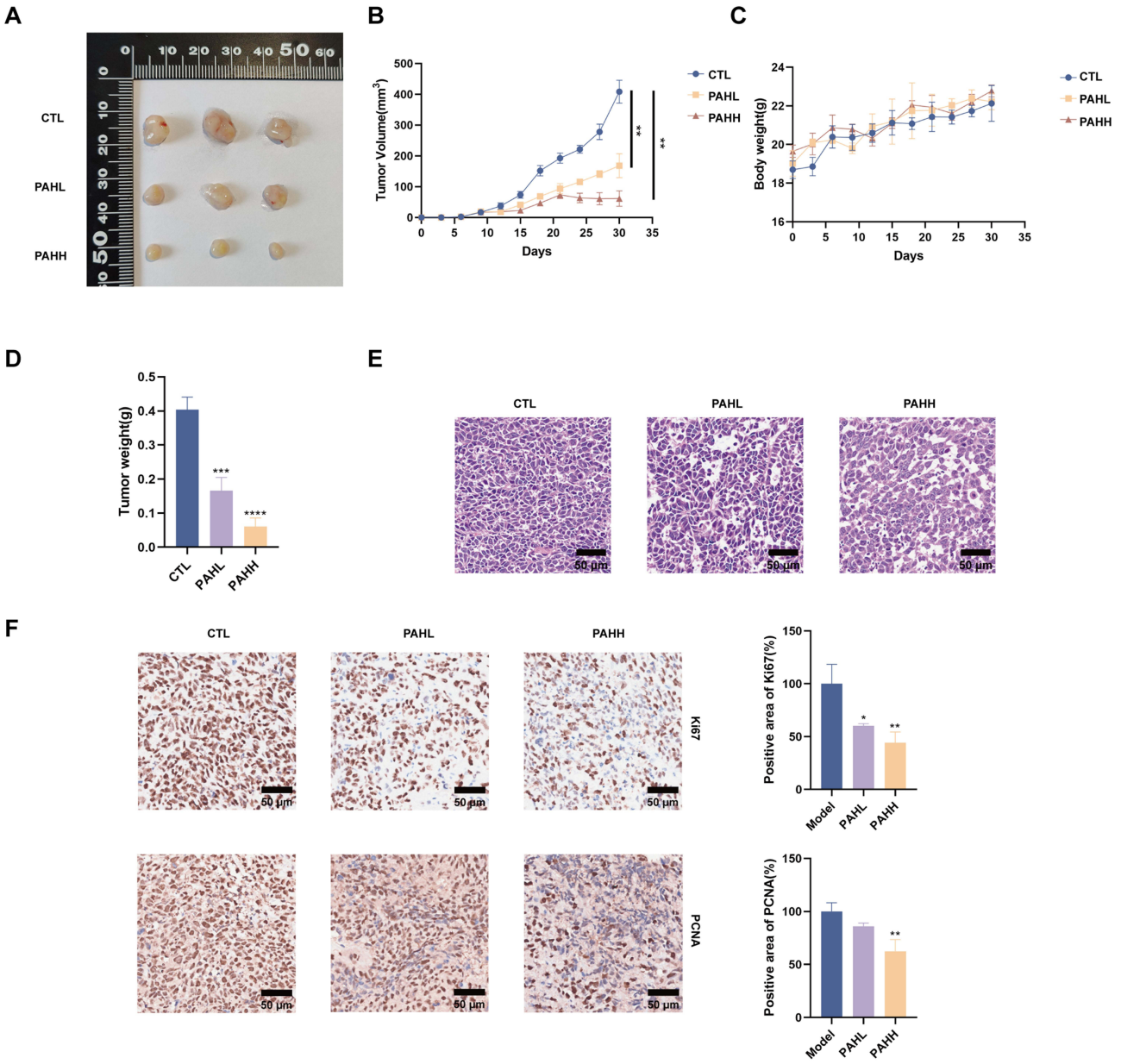

Figure 3 PAH inhibits the progression of CRC in vivo. (**A**) Stereophotos of xenograft tumors in mice given PAH or a vehicle control for treatment. The growth curves of tumor volume are shown in (B). (**C**) The paths of bodily weight. (**D**) A graph displaying the weights of each tumor. (**E**) Histo-embedded staining of single tumors. (**F**) Pictures of Ki67 and PCNA stained by IHC. All data were expressed as mean ± SD. *P < 0.05, **P < 0.01, ***P < 0.001, ****P < 0.0001.

(Figure 4A). Comprehensive gene set enrichment analysis (GSEA) analysis underscored the importance of autophagy in PAH's mechanism, as demonstrated by changes in autophagy-related gene expression (Figure 4B and C). The impact of PAH on cell viability was further evaluated by co-administering ferrostatin-1 (1 μM), Pifithrin-α (20 μM), and chloroquine (10 μM) with PAH (Figure 4D). While inhibitors of ferroptosis and p53 had no significant effect on PAH's activity, the addition of an autophagy inhibitor reversed PAH's suppressive effects on CRC cell lines.

PAH Induces Autophagy of CRC Cells

To assess whether PAH triggers autophagy in CRC cells, we conducted transmission electron microscopy (TEM) to detect autophagic vacuoles. Observations confirmed the formation of autophagic vacuoles in both HCT116 and SW480 cells post-PAH exposure, verifying autophagy induction (Figure 5A). Additionally, we evaluated the autophagy markers

https://doi.org/10.2147/DDDT.S525006

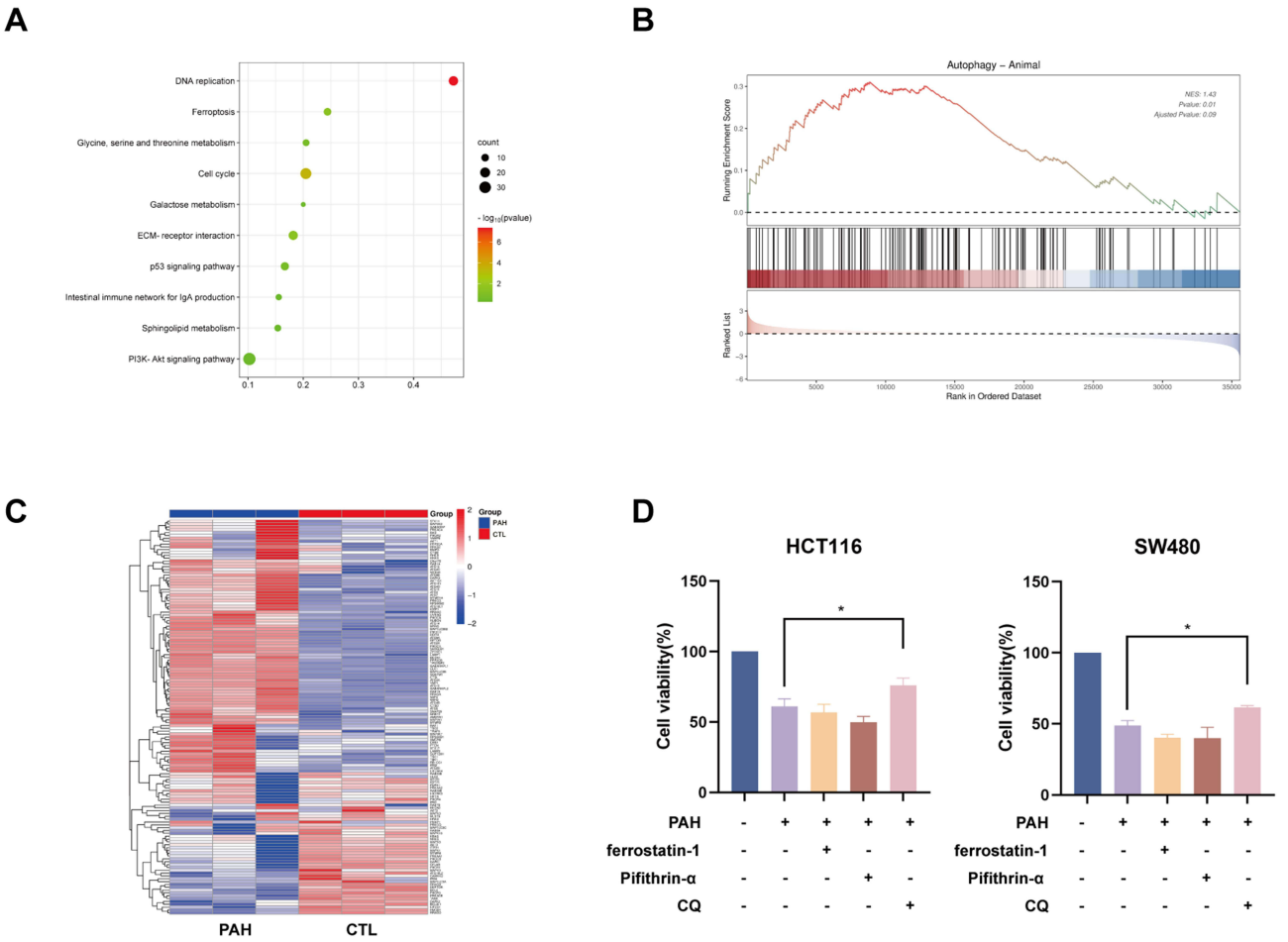

Figure 4 RNA-seq analysis. (**A**) Analysis of KEGG pathway enrichment. (**B**) Result of GSEA. (**C**) Heatmap displaying significant expression differences in autophagy-related genes between PAH-treated and control groups. (**D**) Cell viability measured using a CCK-8 kit after treatment with ferrostatin-1, Pifithrin-α, chloroquine, and PAH for 24 hours. All data were expressed as mean ± SD. *P < 0.05.

LC3B and P62 using WB analysis, which revealed an increase in LC3B-II and a decrease in P62 across both cell lines in a dose-dependent manner (Figure 5B). IF studies showed that the fluorescence intensity of LC3B-II rose with increasing PAH concentrations (Figure 5C). The application of the autophagy inhibitor chloroquine (CQ) indicated that simultaneous treatment with CQ and PAH enhanced the accumulation of LC3B-II and P62, suggesting increased autophagic activity (Figure 5D).

PAH Inhibits PI3K/AKT Pathway to Regulate CRC Cell Autophagy

We used WB to quantify the amounts of PI3K and AKT, as well as their phosphorylated forms, to study its involvement in PAH-induced autophagy. As the dosage of PAH increased, we found that the p-PI3K/PI3K and p-AKT/AKT ratios rose as well (Figure 6A). In contrast, in normal epithelial cells such as NCM460, the relatively low baseline activity of the PI3K/AKT pathway and low expression of SRD5A1 (Supplementary Figure 1B) may account for the observation that 200 μM PAH induces only moderate and self-limiting protective autophagy, without reaching the threshold necessary to trigger autophagic cell death (Supplementary Figure 1C).

Silencing PTEN with siRNA markedly attenuated the PAH-induced autophagic response in CRC cells, as evidenced by diminished LC3B-II accumulation (Supplementary Figure 1D). Consistently, CCK-8 assays demonstrated that the pro-apoptotic (cytotoxic) effect of PAH was significantly weakened under PTEN knockdown (Supplementary Figure 1E). Conversely, pharmacological blockade of the PI3K/AKT axis—using the PI3K inhibitor LY294002 (Figure 6B) or the

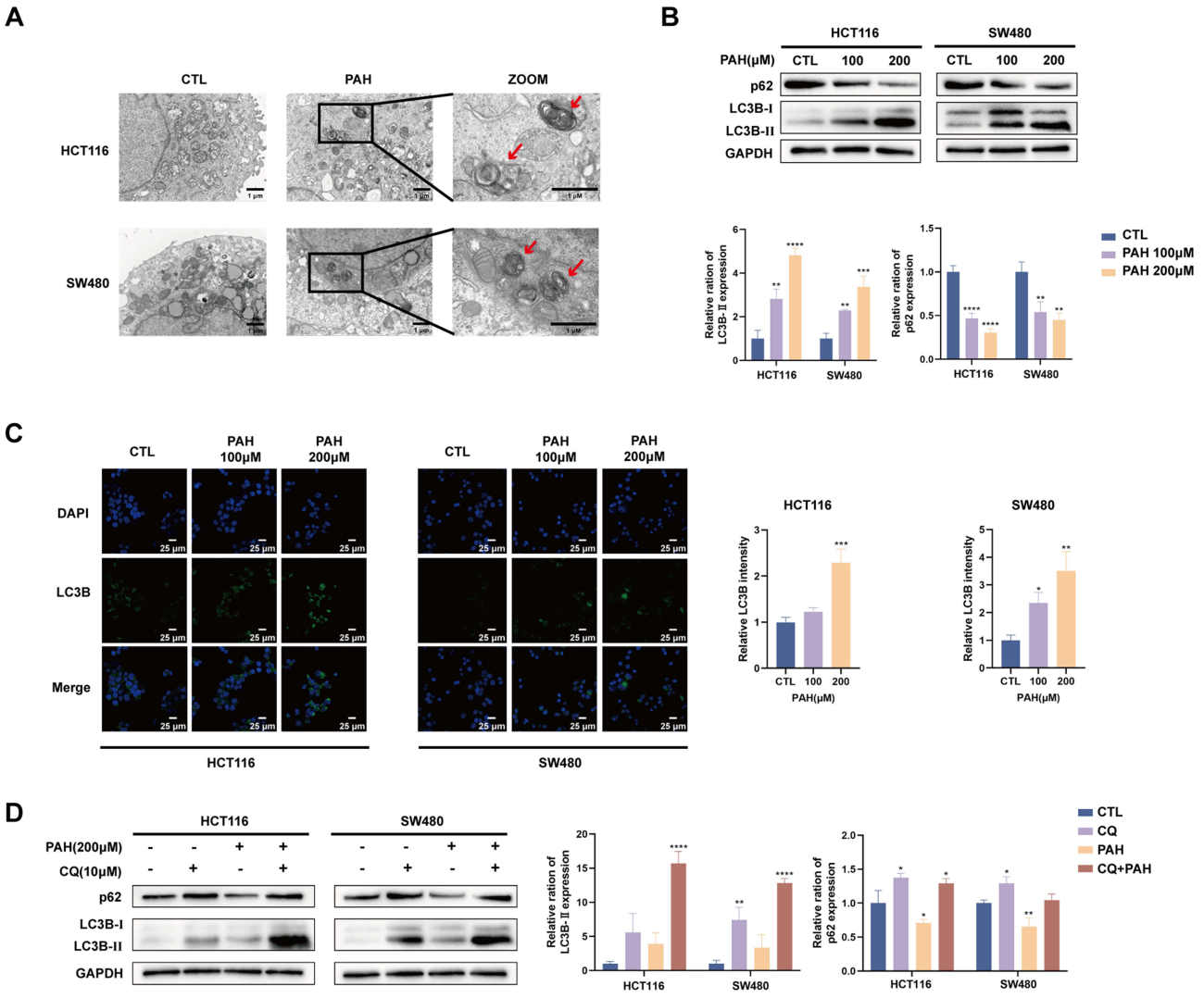

Figure 5 PAH induces autophagy of CRC cells. (A)TEM revealed autophagic vacuoles in cells treated with 200 μM PAH, marked by red arrows. (**B**) Variations in LC3B and P62 levels were monitored in HCT116 and SW480 cells treated with different concentrations of PAH. (**C**) IF highlighted endogenous LC3B puncta in cells after 24 hours of PAH treatment. (**D**) Levels of LC3 and P62 were analyzed in cells co-treated with PAH and CQ (10 μM). All data were expressed as mean ± SD. *P < 0.05, **P < 0.01, ***P < 0.001, ****P < 0.0001.

AKT inhibitor MK-2206 (Supplementary Figure 1F)—robustly augmented LC3B-II levels while reducing p62 expression in PAH-treated cells, indicating potentiated autophagic flux.

PAH Targets SRD5A1 to Promote Autophagy via PI3K/AKT Pathway

To discern PAH's potential targets, we employed the SwissTargetPrediction tool. Figure 7A illustrates the principal targets, highlighting SRD5A1 as possessing the utmost binding likelihood. We employed molecular docking to anticipate interactions between the compound and its protein targets.[22] Investigations into SRD5A1 demonstrated that PAH formed hydrogen bonds with HIS-94, ARG-98, and GLU-202 in the domain, registering a docking affinity of −5.7 kcal/mol, signifying robust binding affinity (Figure 7B). Confirmation of these docking results came from molecular dynamics simulations, depicted in Figure 7C. RMSD serves as a vital stability indicator, where lower values denote greater stability of the complex.[23] The average RMSD of the PAH-SRD5A1 complex was recorded under 0.4 nm, with fluctuations stabilizing under 0.2 nm post-30 ns, affirming system stability and docking result validity. To verify if PAH modulates its anticancer effects through SRD5A1, WB experiments were carried out on CRC cell lines exposed to PAH. Results from Figure 7D show that SRD5A1 protein levels in the treated cells were significantly lower. Validation of target engagement

https://doi.org/10.2147/DDDT.S525006

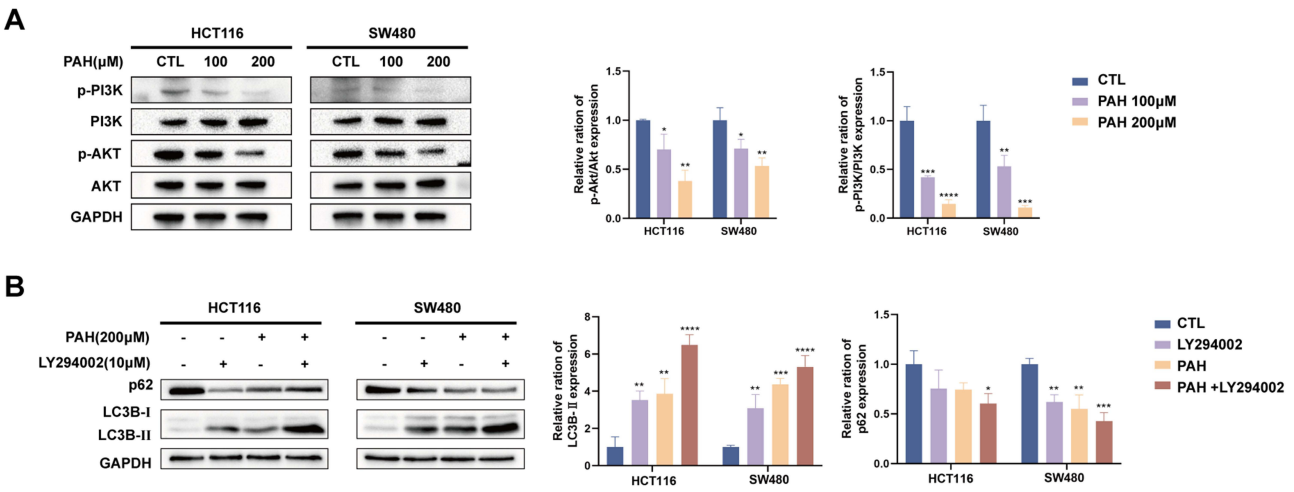

Figure 6 PAH inhibits PI3K/AKT signaling pathway to regulate CRC cell autophagy. (**A**) Levels of AKT, p-AKT, PI3K, and p-PI3K were assessed in HCT116 and SW480 cells treated with various concentrations of PAH. (**B**) Levels of LC3 and P62 were measured following treatment with PAH and LY294002 (10 μM). All data were expressed as mean ± SD. *P < 0.05, **P < 0.01, ***P < 0.001, ****P < 0.0001.

was performed using a cellular thermal shift assay, which revealed that HCT116 and SW480 cells treated with PAH demonstrated superior thermal stability of the SRD5A1 complex compared to the control (Figure 7E). Associations between elevated SRD5A1 levels and the severity of various cancers have been documented. To probe SRD5A1's biological roles in CRC, we examined its expression in cancerous and adjacent non-cancerous tissues across a spectrum of cancers via the TCGA database. Figure 7F shows significant upregulation of SRD5A1 in diverse cancer tissues, notably in colon adenocarcinoma (COAD) and rectum adenocarcinoma (READ). Furthermore, comparative analyses of SRD5A1 levels between CRC patients (n=275) and healthy subjects (n=349) revealed pronounced elevations in CRC samples (Figure 7G). Moreover, the diagnostic ROC curve confirms a high predictive accuracy of SRD5A1 for CRC diagnosis (Figure 7H). Investigating how PAH affects CRC by targeting SRD5A1, we sourced the GSE147456 dataset from the GEO database. This dataset, a comparative transcriptomic assessment between HCT116 cells with SRD5A1 suppression and controls, indicated that PAH potentially influences CRC by modulating the PI3K/AKT pathway (Figure 7I). Studies suggest that SRD5A1 inhibition in multiple myeloma may attenuate the PI3K/AKT pathway and foster autophagy, thereby hindering tumorigenesis.[24] To substantiate these results, we employed dutasteride, an SRD5A1 inhibitor. WB tests showed that simultaneous treatment with dutasteride curtailed the PI3K/AKT pathway and escalated autophagic activity, thus triggering autophagy (Figure 7J–7K).

Discussion

In our research, we explored PAH, the key active component in perilla essential oil and a volatile monoterpene, known for its negligible side effects and acknowledged safety by the US Food and Drug Administration and the Flavor and Extract Manufacturers Association.[25] Zhang et al[26] reported PAH's ability to inhibit gastric cancer growth through autophagy induction. Lin et al noted PAH's potential to suppress prostate cancer progression and affect stem cell characteristics. Furthermore, Catanzaro et al[27] highlighted PAH's induction of anti-leukemia activity via the ferroptosis pathway. Considering PAH's anticancer capabilities, our assessments confirmed its anti-CRC properties, supporting the potential development of PAH as an effective anti-CRC therapeutic.

In our research, PAH was found to exert potent anti-proliferative and pro-apoptotic effects on CRC cells. Notably, at concentrations up to 200 μM, PAH exhibited minimal cytotoxicity toward NCM460. This selective cytotoxicity is consistent with previous studies indicating that PAH has a preferential impact on malignant cells.[28,29] Our own viability assays further support this observation, with the IC_{50} of PAH for NCM460 being approximately 576.9 μM—substantially higher than the IC_{50} values observed in CRC cell lines HCT116 (239.4 μM) and SW480 (218.9 μM). These data suggest that the PAH concentration effective in targeting tumor cells remains below the toxicity threshold for normal epithelial cells.

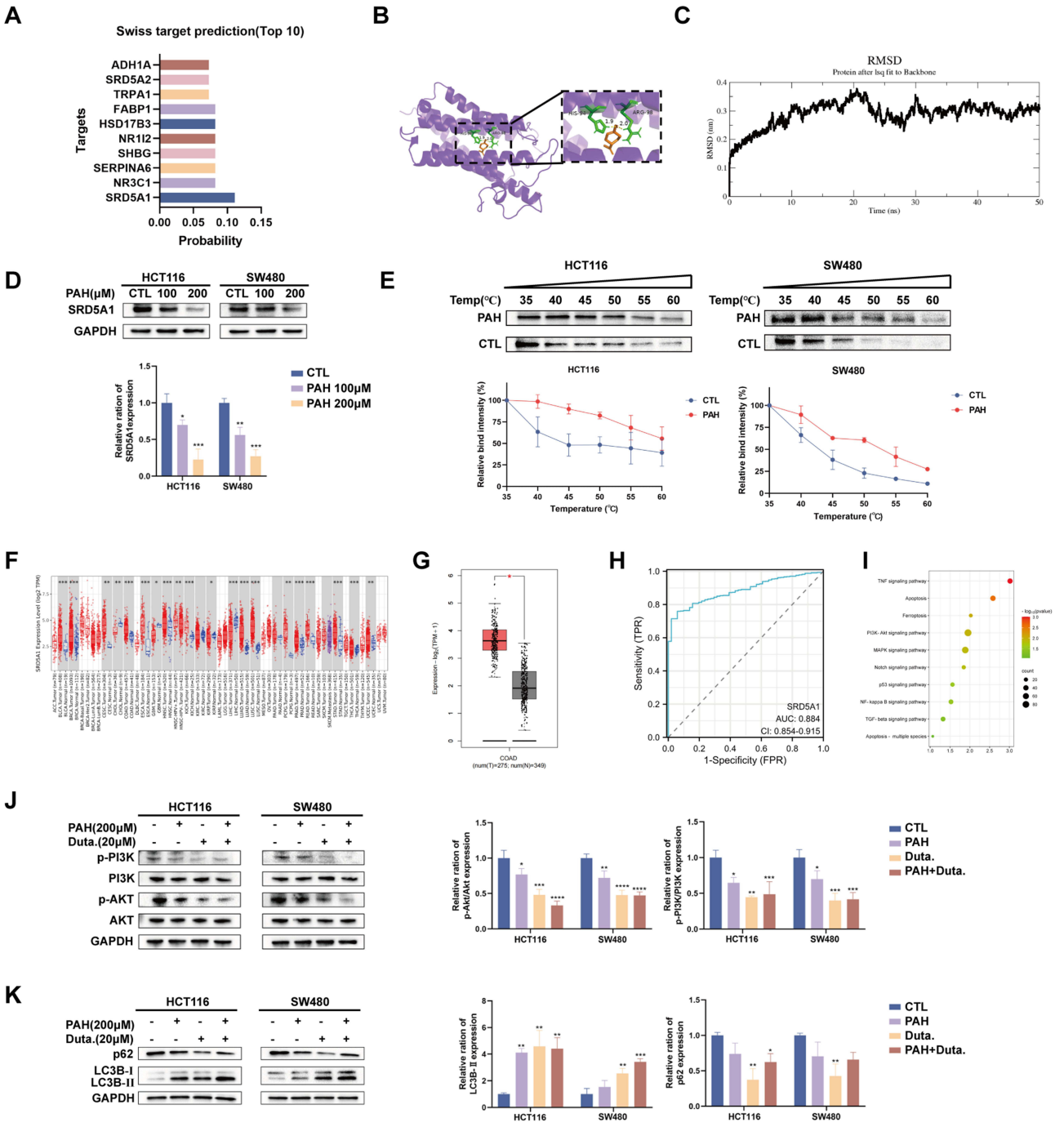

Figure 7 The potential targets of PAH. (**A**) Swiss Target Prediction identifies the top ten likely macromolecular targets of PAH. (**B**) Modeling predicts interactions between PAH and SRD5A1. (**C**) Analysis of molecular dynamics simulations examining the PAH-SRD5A1 interaction. (**D**) WB determined SRD5A1 expression levels. (**E**) The CETSA method evaluated the binding affinity of PAH for SRD5A1 in HCT116 and SW480 cells across different temperatures. (**F**) Analysis of SRD5A1's differential expression in various cancers, using the TCGA database. (**G**) Expression disparity of SRD5A1 between tumor (T) and matched normal (N) tissues in COAD, as analyzed in GEPIA2. (**H**) Diagnostic ROC curve analysis. (**I**) Investigation into KEGG pathway enrichment using GSE147456 dataset. (**J**) After co-incubating cells with PAH with or without dutasteride (20 μm), levels of AKT, p-AKT, PI3K, p-PI3K were evaluated. (**K**) Following incubation with PAH and dutasteride (20 μm), levels of LC3 and p62 were assessed. All data were expressed as mean ± SD. *P < 0.05, **P < 0.01, ***P < 0.001, ****P < 0.0001.

To further delineate the mechanisms through which PAH facilitates CRC treatment, transcriptomic approaches were employed to forecast its likely actions. KEGG enrichment analysis indicates PAH's involvement in pathways like ferroptosis and p53. Although the autophagy pathway appeared underexpressed in KEGG analyses, GSEA suggested a substantial role for autophagy in mediating the therapeutic impact of PAH on CRC. Co-administration of pathway-

https://doi.org/10.2147/DDDT.S525006

specific inhibitors with PAH revealed that an autophagy inhibitor reversed PAH's inhibitory effects on CRC cell proliferation. Autophagy, a conserved cellular self-digestion process in eukaryotic organisms,[30] involves the fusion of autophagosomes with lysosomes to create autolysosomes, removing old and damaged organelles and recycling their components to maintain cellular equilibrium and renewal.[31] Given autophagy's complex role in tumor dynamics, stimulating autophagy is regarded as a promising strategy for CRC management. Our investigations showed a significant elevation in LC3B fluorescence and autophagic flux following PAH treatment. Chloroquine (CQ), a late-stage autophagy inhibitor, impedes the amalgamation of autophagosomes and lysosomes, effectively stalling autophagic processes.[32] Assessments using CQ to monitor autophagic flux demonstrated that PAH intensifies autophagic activity compared to treatment with CQ alone, implying that PAH initiates and promotes autophagosome breakdown. Autophagy is influenced by several molecular mechanisms, with the PI3K/AKT pathway serving a crucial regulatory function in its initiation and progression. Further investigation revealed that the PI3K/AKT pathway, a critical regulator of autophagy, is a key target of PAH. Western blot analysis showed that PAH treatment significantly reduced phosphorylation of PI3K and AKT. Co-treatment with LY294002, a PI3K inhibitor, further amplified autophagic markers, supporting the conclusion that PAH-induced autophagy is mediated via PI3K/AKT suppression. Except for LY294002, other inhibitors (MK-2206) or inhibitory factors (such as PTEN) within the PI3K/Akt pathway can have similar effects.

We subsequently employed bioinformatics to propose that PAH's anticancer effects derive from its targeting and inhibition of SRD5A1, with initial validations following. SRD5A1 is predominantly expressed in the skin[33] and has associations with various cancer forms.[24,34–36] Wei et al[35] revealed that SRD5A1 affects CRC cell viability and triggers apoptosis, thereby establishing it as a potential biomarker for CRC diagnosis and prognosis. Our results indicate that PAH targets and suppresses SRD5A1, modulates the PI3K/AKT pathway, and induces autophagy, underscoring its potential as a CRC therapeutic. Mechanistically, SRD5A1, the direct target of PAH, is expressed at much lower levels in NCM460 compared to CRC cells, and the basal activity of the PI3K/AKT pathway is also lower. Moreover, PAH-induced autophagy in NCM460 appears to be moderate and cytoprotective, without triggering autophagic cell death. These findings collectively indicate that PAH preferentially targets tumor cells while sparing normal tissues.

PAH, when considered for CRC treatment, reveals drug efficacy limitations as reflected by its IC_{50} measurements; 265.0 μM for HCT116 and 240.2 μM for SW480. To bypass these constraints and boost therapeutic effectiveness, PAH is proposed as a primary compound for structural enhancement and the creation of more effective derivatives. Notably, the 1,2-epoxy derivative of PAH, synthesized by Andrade, exhibited increased cytotoxicity against CRC cell lines, recording an IC_{50} of 16.14 μM for HCT116. This improvement suggests that introducing an epoxy group to PAH could amplify its biological impact.[37]

Conclusion

In conclusion, our study demonstrates that PAH exerts anti-colorectal cancer activity by targeting SRD5A1, leading to suppression of the PI3K/AKT pathway and induction of autophagy. In vivo and in vitro experiments confirmed its anti-proliferative and pro-apoptotic effects. Moreover, bioinformatics analysis revealed that SRD5A1 is significantly upregulated in CRC tissues, and ROC curve analysis indicated strong diagnostic value. These findings highlight the potential of PAH as a promising candidate for CRC therapy and suggest SRD5A1 as both a therapeutic target and biomarker.

Abbreviations

AKT, Protein Kinase B; CQ, Chloroquine; Duta., Dutasteride; CRC, Colorectal cancer; GEO, Gene expression omnibus; GSEA, Gene set enrichment analysis; KEGG, Kyoto Encyclopedia of Genes and Genomes; PAH, Perillaldehyde; PI3K, Phosphatidylinositol 3 Kinase; SRD5A1, Steroid 5 Alpha Reductase 1.

Ethical Approval and Consent to Participate

This study was performed in line with the principles of the Declaration of Helsinki, and has been approved by the Medical Ethics Committee of Xiamen University (Approval No. XMULAC20240001).

Acknowledgments

We gratefully acknowledge Dongfang Hospital and Xiamen University School of Medicine for providing experimental facilities, and the Naval Medical University for their support with bioinformatics analysis.

Disclosure

The author(s) report no conflicts of interest in this work.

References

1. Dekker E, Tanis PJ, Vleugels JLA, Kasi PM, Wallace MB. Colorectal cancer. *Lancet*. 2019;394(10207):1467–1480. doi:10.1016/S0140-6736(19)32319-0
2. Bray F, Ferlay J, Soerjomataram I, Siegel RL, Torre LA, Jemal A. Global cancer statistics 2018: GLOBOCAN estimates of incidence and mortality worldwide for 36 cancers in 185 countries. *CA Cancer J Clin*. 2018;68:394–424. doi:10.3322/caac.21492
3. Murphy N, Moreno V, Hughes DJ, et al. Lifestyle and dietary environmental factors in colorectal cancer susceptibility. *Mol Aspects Med*. 2019;69:2–9. doi:10.1016/j.mam.2019.06.005
4. Keum N, Giovannucci E. Global burden of colorectal cancer: emerging trends, risk factors and prevention strategies. *Nat Rev Gastroenterol Hepatol*. 2019;16(12):713–732. doi:10.1038/s41575-019-0189-8
5. Yang L, Atakhanova N, Arellano MTC, et al. Translational research of new developments in targeted therapy of colorectal cancer. *Pathol Res Pract*. 2023;252:154888. doi:10.1016/j.prp.2023.154888
6. Johdi NA, Sukor NF, Hu L, Qiu L, Zhu L. Colorectal Cancer Immunotherapy: options and Strategies. *Front Immunol*. 2020;11:11. doi:10.3389/fimmu.2020.00011
7. He Y, Sun MM, Zhang GG, et al. Targeting PI3K/Akt signal transduction for cancer therapy. *Signal Transduct Target Ther*. 2021;6(1):425. doi:10.1038/s41392-021-00828-5
8. Danielsen SA, Eide PW, Nesbakken A, Guren T, Leithe E, Lothe RA. Portrait of the PI3K/AKT pathway in colorectal cancer. *Biochimica Et Biophysica Acta*. 2015;1855(1):104–121.
9. Świechowski R, Pietrzak J, Wosiak A, Mik M, Balcerczak E. Genetic Insights into colorectal cancer: evaluating PI3K/AKT signaling pathway genes expression. *Int J Mol Sci*. 2024;25(11):5806. doi:10.3390/ijms25115806
10. Levine B, Kroemer G. Autophagy in the pathogenesis of Disease. *Cell*. 2008;132(1):27–42. doi:10.1016/j.cell.2007.12.018
11. Zhang Y, Li H, Lv L, et al. Autophagy: dual roles and perspective for clinical treatment of colorectal cancer. *Biochimie*. 2023;206:49–60. doi:10.1016/j.biochi.2022.10.004
12. Kimmelman AC. The dynamic nature of autophagy in cancer. *Genes Dev*. 2011;25(19):1999–2010. doi:10.1101/gad.17558811
13. Qian Q, Zhou H, Chen Y, et al. VMP1 related autophagy and apoptosis in colorectal cancer cells: VMP1 regulates cell death. *Biochem Biophys Res Commun*. 2014;443(3):1041–1047. doi:10.1016/j.bbrc.2013.12.090
14. Zhong J, Ding S, Zhang X, et al. To investigate the occurrence and development of colorectal cancer based on the PI3K/AKT/mTOR signaling pathway. *Front Biosci*. 2023;28(2):37. doi:10.31083/j.fbl2802037
15. Galluzzi L, Pietrocola F, Bravo San Pedro JM, et al. Autophagy in malignant transformation and cancer progression. *EMBO J*. 2015;34(7):856–880. doi:10.15252/embj.201490784
16. Wu X, Dong S, Chen H, Guo M, Sun Z, Luo H. Perilla frutescens: a traditional medicine and food homologous plant. *Chin Herb Med*. 2023;15(3):369–375. doi:10.1016/j.chmed.2023.03.002
17. Lin Z, Huang S, Ling Hu X, et al. Perillaldehyde inhibits bone metastasis and receptor activator of nuclear factor-κB ligand (RANKL) signaling-induced osteoclastogenesis in prostate cancer cell lines. *Bioengineered*. 2022;13(2):2710–2719. doi:10.1080/21655979.2021.2001237
18. Elegbede JA, Flores R, Wang RC. Perillyl alcohol and perillaldehyde induced cell cycle arrest and cell death in BroTo and A549 cells cultured in vitro. *Life Sci*. 2003;73(22):2831–2840. doi:10.1016/S0024-3205(03)00701-X
19. Uemura T, Yashiro T, Oda R, et al. Intestinal anti-inflammatory activity of perillaldehyde. *J Agric Food Chem*. 2018;66(13):3443–3448. doi:10.1021/acs.jafc.8b00353
20. Chen L, Wang F, Qu S, et al. Therapeutic potential of perillaldehyde in ameliorating vulvovaginal candidiasis by reducing vaginal oxidative stress and apoptosis. *Antioxidants*. 2022;11(2):178. doi:10.3390/antiox11020178
21. Chu Z, Li Y, Wang L, Wei S, Yang S, Zeng H. Perillaldehyde: a promising antibacterial agent for the treatment of pneumonia caused by Acinetobacter baumannii infection. *Int Immunopharmacol*. 2024;126:111311. doi:10.1016/j.intimp.2023.111311
22. Lu X, Yan G, Dawood M, et al. A novel moniliformin derivative as pan-inhibitor of histone deacetylases triggering apoptosis of leukemia cells. *Biochem Pharmacol*. 2021;194:114677. doi:10.1016/j.bcp.2021.114677
23. Qiao X, Wu X, Chen S, Niu MM, Hua H, Zhang Y. Discovery of novel and potent dual-targeting AXL/HDAC2 inhibitors for colorectal cancer treatment via structure-based pharmacophore modelling, virtual screening, and molecular docking, molecular dynamics simulation studies, and biological evaluation. *J Enzyme Inhib Med Chem*. 2024;39(1):2295241. doi:10.1080/14756366.2023.2295241
24. Dou R, Qian J, Wu W, et al. Suppression of steroid 5alpha-reductase type I promotes cellular apoptosis and autophagy via PI3K/Akt/mTOR pathway in multiple myeloma. *Cell Death Dis*. 2021;12(2):206. doi:10.1038/s41419-021-03510-4
25. Tang LF, Ma X, Xie LW, et al. Perillaldehyde mitigates ionizing radiation-induced intestinal injury by inhibiting ferroptosis via the Nrf2 signaling pathway. *Mol Nutr Food Res*. 2023;67(19). doi:10.1002/mnfr.202300232.
26. Zhang Y, Liu S, Feng Q. Perilaldehyde activates AMP-activated protein kinase to suppress the growth of gastric cancer via induction of autophagy. *J Cell Biochem*. 2019;120(2):1716–1725. doi:10.1002/jcb.27491
27. Hale AN, Ledbetter DJ, Gawriluk TR, Rucker, III EB. Autophagy. *Autophagy*. 2013;9(7):951–972. doi:10.4161/auto.24273
28. Hobbs CA, Taylor SV, Beevers C, et al. Genotoxicity assessment of the flavouring agent, perillaldehyde. *Food Chem Toxicol*. 2016;97:232–242. doi:10.1016/j.fct.2016.08.029

29. Catanzaro E, Turrini E, Kerre T, et al. Perillaldehyde is a new ferroptosis inducer with a relevant clinical potential for acute myeloid leukemia therapy. *Biomed Pharmacother*. 2022;154:113662. doi:10.1016/j.biopha.2022.113662
30. Li H, Li X, Xia R, Zhang X, Jin T, Zhang H. PHGDH knockdown increases sensitivity to SR1, an aryl hydrocarbon receptor antagonist, in colorectal cancer by activating the autophagy pathway. *FEBS J*. 2024;291(8):1780–94.
31. Wu Z, Zhang W, Chen L, et al. CDK12 inhibition upregulates ATG7 triggering autophagy via AKT/FOXO3 pathway and enhances anti-PD-1 efficacy in colorectal cancer. *Pharmacol Res*. 2024;201:107097. doi:10.1016/j.phrs.2024.107097
32. Kocak M, Ezazi Erdi S, Jorba G, et al. Targeting autophagy in disease: established and new strategies. *Autophagy*. 2022;18(3):473–495. doi:10.1080/15548627.2021.1936359
33. Thigpen AE, Silver RI, Guileyardo JM, Casey ML, McConnell JD, Russell DW. Tissue distribution and ontogeny of steroid 5 alpha-reductase isozyme expression. *J Clin Invest*. 1993;92(2):903–910. doi:10.1172/JCI116665
34. Kapp FG, Sommer A, Kiefer T, Dölken G, Haendler B. 5-alpha-reductase type I (SRD5A1) is up-regulated in non-small cell lung cancer but does not impact proliferation, cell cycle distribution or apoptosis. *Cancer Cell Int*. 2012;12(1):1. doi:10.1186/1475-2867-12-1
35. Wei R, Zhong S, Qiao L, et al. Steroid 5α-reductase type I induces cell viability and migration via nuclear factor-κB/vascular endothelial growth factor signaling pathway in colorectal cancer. *Front Oncol*. 2020;10:10. doi:10.3389/fonc.2020.00010
36. Thomas LN, Douglas RC, Rittmaster RS, Too CKL. Overexpression of 5α-reductase type 1 increases sensitivity of prostate cancer cells to low concentrations of testosterone. *Prostate*. 2009;69(6):595–602. doi:10.1002/pros.20911
37. Andrade LN, Severino P, Amaral RG. Evaluation of cytotoxic and antitumor activity of perillaldehyde 1,2-epoxide. *J Med Plant Res*. 2018;12(30):590–600. doi:10.5897/JMPR2018.6699